Na$_v$1.1 Modulation by a Novel Triazole Compound Attenuates Epileptic Seizures in Rodents

John Gilchrist,[†] Stacey Dutton,[‡] Marcelo Diaz-Bustamante,[§] Annie McPherson,[‡] Nicolas Olivares,[§] Jeet Kalia,[||] Andrew Escayg,*[,‡] and Frank Bosmans*[,†,⊥]

[†]Department of Physiology, Johns Hopkins University, School of Medicine, Baltimore, Maryland 21205, United States

[‡]Department of Human Genetics, Emory University, School of Medicine, Atlanta, Georgia 30022, United States

[§]Lieber Institute for Brain Development, Johns Hopkins University, School of Medicine, Baltimore, Maryland 21205, United States

[||]Indian Institute of Science Education and Research Pune, Pune, Maharashtra 411 008, India

[⊥]Solomon H. Snyder Department of Neuroscience, Johns Hopkins University, School of Medicine, Baltimore, Maryland 21205, United States

S Supporting Information

ABSTRACT: Here, we report the discovery of a novel anticonvulsant drug with a molecular organization based on the unique scaffold of rufinamide, an anti-epileptic compound used in a clinical setting to treat severe epilepsy disorders such as Lennox-Gastaut syndrome. Although accumulating evidence supports a working mechanism through voltage-gated sodium (Na$_v$) channels, we found that a clinically relevant rufinamide concentration inhibits human (h)Na$_v$1.1 activation, a distinct working mechanism among anticonvulsants and a feature worth exploring for treating a growing number of debilitating disorders involving hNa$_v$1.1. Subsequent structure−activity relationship experiments with related N-benzyl triazole compounds on four brain hNa$_v$ channel isoforms revealed a novel drug variant that (1) shifts hNa$_v$1.1 opening to more depolarized voltages without further alterations in the gating properties of hNa$_v$1.1, hNa$_v$1.2, hNa$_v$1.3, and hNa$_v$1.6; (2) increases the threshold to action potential initiation in hippocampal neurons; and (3) greatly reduces the frequency of seizures in three animal models. Altogether, our results provide novel molecular insights into the rational development of Na$_v$ channel-targeting molecules based on the unique rufinamide scaffold, an outcome that may be exploited to design drugs for treating disorders involving particular Na$_v$ channel isoforms while limiting adverse effects.
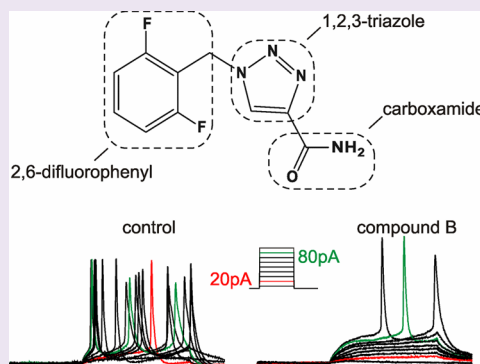
S evere epileptic disorders such as Lennox-Gastaut syndrome (LGS) are commonly associated with various types of seizures and cognitive dysfunction that persist into adulthood.[1] As a result, these patients suffer from varying degrees of learning disabilities, psychiatric disorders, and behavioral abnormalities that can drastically affect their social integration.[1] Diagnosis and subsequent management of LGS are challenging, relying mostly on the expertise of the physician to interpret an intricate amalgamation of clinical and EEG abnormalities.[2] Although limited clinical trials suggest that a small subset of available anti-epileptic drugs (AEDs) such as lamotrigine, valproic acid, topiramate, felbamate, and clobazam may be used to manage the multiple seizure types associated with LGS, their efficacy is often inadequate, and perilous adverse effects may occur.[2] The relatively new drug rufinamide, a compound with orphan drug status in the United States and marketing authorization in Europe, displays a broad spectrum of anti-epileptic activity, and clinical trials have shown long-term beneficial effects and good tolerability when rufinamide is used as adjunctive therapy in children and adults suffering from LGS.[3,4] As such, rufinamide is poised to replace the more

adverse effect-prone classical AEDs as a valuable treatment for LGS[5] as well as partial[3] or refractory focal[6] seizures. Interestingly, the hydrophobic triazole-derived molecular structure of rufinamide is unlike that of any other anti-epileptic compound;[4] nonetheless, the drug is absorbed extensively when taken orally, and dosages of up to 3200 mg/day are common.[4,7,8]

Given their unique role in electrical signaling[9] and subsequent implications in various epilepsy disorders,[10−14] voltage-gated sodium (Na$_v$) channels within the central nervous system (CNS) may be influenced by rufinamide;[15,16] however, it is unclear whether modulating a particular isoform constitutes the primary mode of action. Of the nine Na$_v$ channel isoforms (Na$_v$1.1−Na$_v$1.9) identified in humans, four are expressed predominantly in the CNS [Na$_v$1.1 (SCN1A), Na$_v$1.2 (SCN2A), Na$_v$1.3 (SCN3A), and Na$_v$1.6 (SCN8A)].[9,17] Supporting their physiological importance, mutations in

Table 1. Effects of 100 μM Rufinamide and Its Derivatives on Human Na$_v$ Channel Isoforms[a]

		hNa$_v$1.1	hNa$_v$1.2	hNa$_v$1.3	hNa$_v$1.6
control	activation ($V_{1/2}$) (mV)	-37.8 ± 1.7	-31.4 ± 1.5	-25.4 ± 1.4	-29.0 ± 2.2
	inactivation ($V_{1/2}$) (mV)	-52.9 ± 1.0	-57.1 ± 0.3	-52.2 ± 0.7	-64.8 ± 1.2
	recovery (T) (ms)	3.4 ± 0.2	6.6 ± 0.5	5.6 ± 0.3	4.4 ± 0.3
DMSO	activation ($V_{1/2}$) (mV)	-38.2 ± 1.9	-31.7 ± 1.2	-24.7 ± 1.6	-26.7 ± 1.1
	inactivation ($V_{1/2}$) (mV)	-49.4 ± 0.3	-59.7 ± 0.4	-52.8 ± 0.9	-65.1 ± 0.8
	recovery (T) (ms)	3.8 ± 0.5	7.1 ± 0.4	6.5 ± 0.3	5.0 ± 0.4
rufinamide	activation ($V_{1/2}$) (mV)	-30.6 ± 0.9*	-29.5 ± 1.2	-24.5 ± 2.4	-28.1 ± 0.8
	inactivation ($V_{1/2}$) (mV)	-47.8 ± 1.6	-57.7 ± 0.5	-52.6 ± 1.6	-60.0 ± 0.7*
	recovery (T) (ms)	5.1 ± 0.2*	10.6 ± 0.3*	9.2 ± 0.5*	7.4 ± 0.3*
		compound A	compound B	compound C	compound D
hNa$_v$1.1	activation ($V_{1/2}$) (mV)	-30.8 ± 1.0*	-27.4 ± 1.0*	-38.4 ± 1.3	-32.5 ± 2.3
	inactivation ($V_{1/2}$) (mV)	-50.5 ± 1.2	-49.4 ± 0.3	-49.2 ± 0.6	-49.8 ± 1.6
	recovery (T) (ms)	4.1 ± 0.5	3.9 ± 0.1	3.1 ± 0.1	3.9 ± 0.3

[a]Drug values are compared to DMSO values for statistical comparison, which is considered significant if the result of the Student's t test indicated a p of <0.005 (denoted with asterisks).

Na$_v$1.1,[12,18,19] Na$_v$1.2,[13] and Na$_v$1.6[20,21] have been linked to various epilepsy phenotypes, whereas Na$_v$1.3 is believed to be involved also in nociception after channel upregulation due to spinal cord injury.[22−24] Consequently, we set out to investigate whether rufinamide influences the functional properties of one or more of these four Na$_v$ channel isoforms. To this end, we transiently expressed human (h) hNa$_v$1.1, hNa$_v$1.2, hNa$_v$1.3, and hNa$_v$1.6 in a robust heterologous expression system and found that a clinically relevant rufinamide concentration primarily influences the voltage dependence of hNa$_v$1.1 activation and availability of hNa$_v$1.6 channels, whereas the recovery from fast inactivation of hNa$_v$1.1, hNa$_v$1.2, hNa$_v$1.3, and hNa$_v$1.6 is only slightly altered. Subsequent experiments with structurally related compounds reveal that chemical derivatization at particular positions on the triazole pharmacophore may be exploited to obtain specific inhibition of hNa$_v$1.1 activation, thereby increasing seizure thresholds in rodent models of epilepsy.

■ RESULTS

Expressing Human Na$_v$ Channel Isoforms in *Xenopus* Oocytes. To identify the molecular target of rufinamide in the brain, we examined potential drug-induced alterations of human neuronal Na$_v$ channel opening and closing (i.e., gating). Although stable cell lines of hNa$_v$1.1, hNa$_v$1.2, hNa$_v$1.3, and hNa$_v$1.6 have been reported,[29−32] DNA rearrangement events and low protein levels have hampered in-depth experiments with these genes in *Xenopus laevis* oocytes, a transient and robust heterologous expression system widely used to address fundamental questions about the gating mechanisms and pharmacological sensitivities of individual ion channel isoforms. By combining careful full-length clone sequencing with transformations of cDNA modified with an ER forwarding motif[25] and the rNa$_v$1.2a 3′UTR region into low-copy *Escherichia coli* variants (CopyCutter EPI400), we were able to consistently obtain robust ionic currents for all four human Na$_v$ channel isoforms in *Xenopus* oocytes (Figure S1 of the Supporting Information). Examination of the G−V relationships for hNa$_v$1.1, hNa$_v$1.2, hNa$_v$1.3, and hNa$_v$1.6 (Figure S1 of the Supporting Information) reveals that the midpoints ($V_{1/2}$) for channel activation are -37.8, -31.4, -25.4, and -36.7 mV, respectively (Table 1). Although the same relative order of midpoints is essentially observed in mammalian cell recordings,[29−32] their absolute values as well as those from channel

availability and recovery from inactivation measurements (Figure S1 of the Supporting Information and Table 1) differ noticeably, yet this observation is not surprising considering the variability in lipid membrane, glycosylation, and auxiliary subunit composition between diverse cell types. Next, we applied rufinamide to hNa$_v$1.1−hNa$_v$1.3 and hNa$_v$1.6 to determine whether the drug alters channel gating.

The Gating Process of Human Na$_v$ Channels Is Altered by Rufinamide. Rufinamide, or 1-[(2,6-difluorophenyl)-methyl]-1H-1,2,3-triazole-4-carboxamide,[4] is slightly soluble in water but dissolves readily in dimethyl sulfoxide (DMSO) at concentrations of up to 9 mg mL^{-1} (Figure 1A). As such, patients are given the drug either as a tablet formulation (Banzel) or as an oral suspension (Inovelon), preferably to be taken with food.[7] On the basis of these properties, we dissolved rufinamide in DMSO and diluted this stock solution with appropriate recording media to a final concentration of 100 μM, thereby approximating clinically observed serum quantities.[4,8,33] Subsequently, Na$_v$ channel-expressing cells were exposed to 100 μM rufinamide in a solution containing at most 1% DMSO. Control experiments without the drug revealed that the gating properties of hNa$_v$1.1, hNa$_v$1.2, hNa$_v$1.3, and hNa$_v$1.6 are not significantly affected upon exposure to 1% DMSO (Figure S2 of the Supporting Information and Table 1). Hereafter, we will consider the gating parameters from DMSO-treated Na$_v$ channel isoforms to be our control values.

After incubating oocytes with 100 μM rufinamide, we observed an ~8 mV depolarizing shift in the G−V relationship of hNa$_v$1.1, whereas the activation of hNa$_v$1.2, hNa$_v$1.3, and hNa$_v$1.6 is not inhibited (Figure 1 and Table 1). In contrast, steady-state inactivation of hNa$_v$1.1, hNa$_v$1.2, and hNa$_v$1.3 is not influenced; however, 100 μM rufinamide does alter the midpoint of hNa$_v$1.6 channel availability by approximately +5 mV (Figure 1 and Table 1). Moreover, recovery from fast inactivation slows for all tested Na$_v$ channel isoforms (Figure 1 and Table 1), and although these effects are subtle, the combination with a substantial shift in hNa$_v$1.1 activation voltage may help explain a decrease in neuronal excitability after administration of the drug.[15] Altogether, our experiments with four neuronal Na$_v$ channel isoforms suggest that rufinamide primarily influences hNa$_v$1.1 and hNa$_v$1.6 function, an observation that supports a role of these particular Na$_v$ channel variants in epilepsy syndromes.[10,12−14,18,20,21] It is worth noting
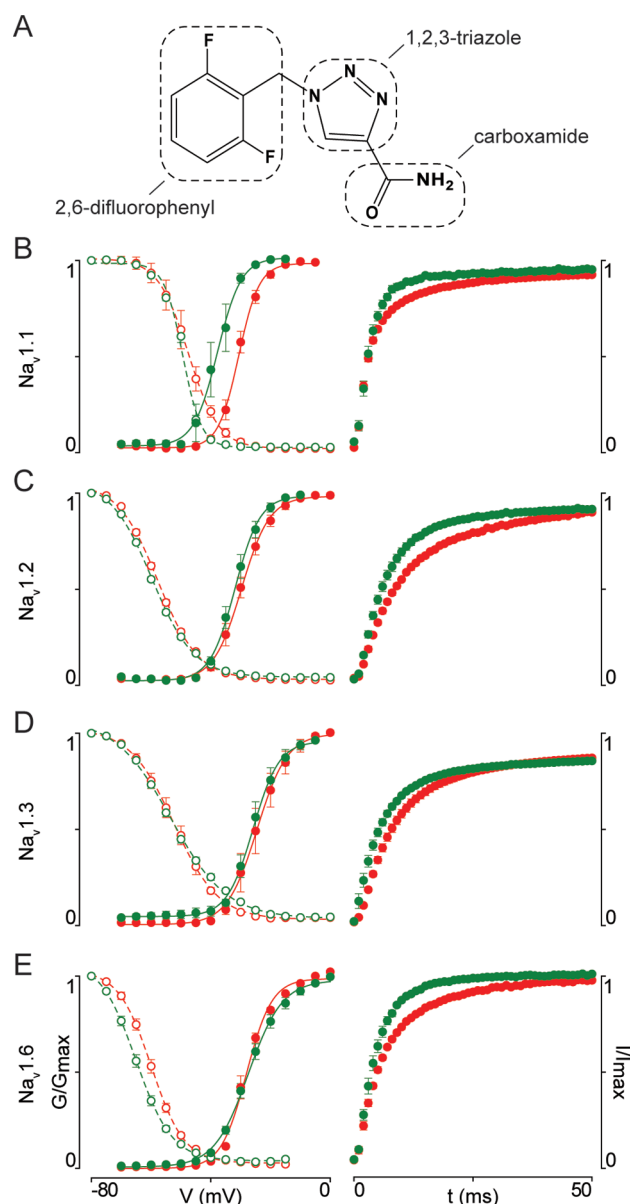
Figure 1. Effect of 100 μM rufinamide on human Na$_v$ channel isoforms involved in epilepsy. (A) Molecular organization of rufinamide consisting of the 1,2,3-triazole ring connecting the 2,6-difluorophenyl and the carboxamide. (B−E) The left column shows G/G_{max} and I/I_{max} relationships, whereas the right column displays the recovery from fast inactivation. The figure shows that rufinamide inhibits hNa$_v$1.1 opening whereas the effect on hNa$_v$1.6 is not significant compared to the effect of DMSO treatment of this particular isoform (see Table 1). Furthermore, the recovery from fast inactivation slows for the four Na$_v$ channel isoforms tested here. All data are shown before (green, DMSO control) and after (red) addition of 100 μM rufinamide to hNa$_v$1.1 (B), hNa$_v$1.2 (C), hNa$_v$1.3 (D), and hNa$_v$1.6 (E). All fit values are listed in Table 1. $n = 5-8$, and error bars represent the standard error of the mean.

that rufinamide may alter hNa$_v$1.1 activation by influencing voltage-sensor activation or by slowing subsequent gating transitions,[34] a distinct working mechanism among the classic anticonvulsant drugs because these compounds are thought to exert their effect by (1) occluding the pore to prevent sodium ion flow or (2) interacting with the inactivated state to decrease the size of the pool of channels available for opening.[33,35−37] Next, we wanted to explore whether particular structural

features of the rufinamide molecule can enhance hNa$_v$1.1 selectivity.

Molecular Modifications of Rufinamide Enhance the Effects on hNa$_v$1.1. The triazole-derived molecular organization of rufinamide is unique among anti-epileptic compounds.[4] To examine which features of the *N*-benzyltriazole core are important for its inhibitory action on hNa$_v$1.1, we performed a structure−activity relationship (SAR) study using four structurally related compounds with unknown functionality: 1-[(3-fluorophenyl)methyl]-1*H*-1,2,3-triazole-4-carboxamide-5-amine (compound A), 1-(phenylmethyl)-1*H*-1,2,3-triazole-4-carboxamide-5-methyl (compound B), 1-[(3-fluorophenyl)methyl]-1*H*-1,2,3-triazole-4-hydroxymethyl (compound C), and 1-[(4-fluorophenyl)methyl]-1*H*-1,2,3-triazole-4-carboxamide-5-amine (compound D). We found that compounds A and B inhibit hNa$_v$1.1 opening (Figure 2 and Table 1) and compound B produces the largest depolarizing shift in channel activation voltage (approximately
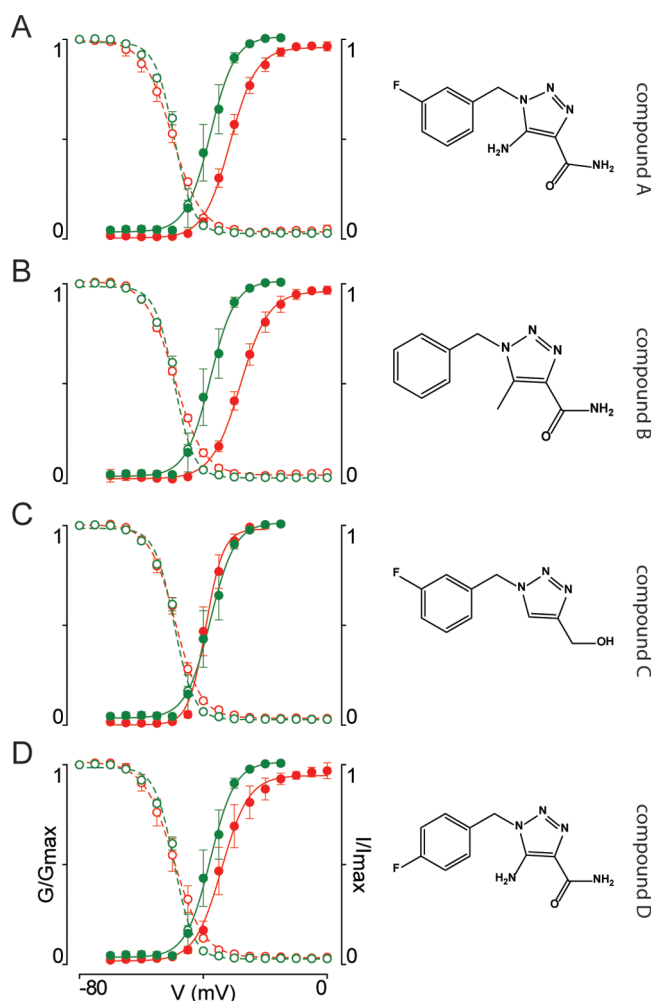

Figure 2. Effect of rufinamide derivatives on hNa$_v$1.1. (A−D) The left column shows G/G_{max} relationships before (green, DMSO control) and after (red) addition of 100 μM rufinamide derivatives fitted with the Boltzmann equation. Compounds A and B clearly inhibit hNa$_v$1.1 opening, whereas compound C no longer affects hNa$_v$1.1 opening (compound D is not significant when considering $p < 0.005$). Fit values are listed in Table 1. $n = 5-8$, and error bars represent the standard error of the mean. The right column displays the molecular organization of the four tested derivatives (compounds A−D).

+11 mV). Strikingly, neither of these compounds influences $hNa_v1.1$ steady-state inactivation, recovery from inactivation, or the persistent current[38] (Figures S3 and S4A,B of the Supporting Information and Table 1), suggesting a working mechanism geared toward stabilizing a closed state of this particular Na_v channel isoform. In contrast to the effect of rufinamide, application of 100 μM compound B selectively modulates $hNa_v1.1$ activation whereas the tested gating parameters of $hNa_v1.2$, $hNa_v1.3$, and $hNa_v1.6$ are unaltered (Figure S5 and Table S1 of the Supporting Information and Table 1). Moreover, our results suggest that rufinamide and compound B do not influence the entry into or voltage dependence of $hNa_v1.1$ slow inactivation (Figure S6 and Table S2 of the Supporting Information).[39] Finally, rufinamide and compound B (100 μM) do not activate the $\alpha1/\beta2/\gamma2$ $GABA_A$ receptor (Figure S4C of the Supporting Information), a subtype ubiquitously found in GABAergic neurons that is targeted by psychoactive drugs such as zolpidem and benzodiazepines.[40] Also, neither drug inhibits hERG,[27] a member of the cardiac potassium channel family and an FDA-mandated screening target for potential off-target drug effects (Figure S7 of the Supporting Information).

One of the most captivating results from our SAR studies is that compound B inhibits $hNa_v1.1$ more efficaciously than rufinamide (Figure 2 and Table 1). The identification of such a molecule is particularly exciting as it underlines the broad scope of rufinamide scaffold-based drug development for treating $hNa_v1.1$-related disorders. Upon comparison of the structures of rufinamide and compound B, two differences stand out. On one hand, rufinamide has two electron-withdrawing fluoro substituents on the phenyl group whereas compound B has none, thereby rendering the phenyl group of this molecule more electron-rich. On the other hand, there is an additional methyl substituent on the triazole ring in compound B, resulting in an increased level of hydrophobic character increased compared to that of rufinamide. Another important observation from our experiments is that compound D has diminished activity whereas compound C no longer influences $hNa_v1.1$ gating at all (Figure 2c). The most significant structural feature of compound C is the presence of a methylene hydroxyl (-CH_2OH) group on its triazole moiety; an amide (-$CONH_2$) substituent is found in the other compounds. To determine whether compound B is physiologically active, we next examined the activity of this molecule in hippocampal neurons.

Compound B Increases the Action Potential Threshold in Hippocampal Neurons. The $Na_v1.1$ distribution is strikingly similar in human and rodent brains.[41] Moreover, 99% of the amino acids that make up $Na_v1.1$ are conserved among humans, rats, and mice (ClustalΩ[42]). As such, we expect the inhibitory effect of compound B to increase the action potential threshold in $Na_v1.1$-expressing rat hippocampal neurons. To test this hypothesis, we applied a physiological solution containing 100 μM compound B to cultured hippocampal neurons and found that a current injection of 80 pA elicits an action potential (Figure 3a). In contrast, hippocampal neurons under control conditions require a current injection of only 20 pA to start generating action potentials (Figure 3A). When assessing average firing thresholds by calculating the potential at which the rate of rise crosses 40 V/s, we observe a value of -43.3 ± 2.4 mV for control cells, whereas a threshold of -27.8 ± 1.6 mV is noted when cells are treated with 100 μM compound B (Figure 3B). Altogether, these results suggest an
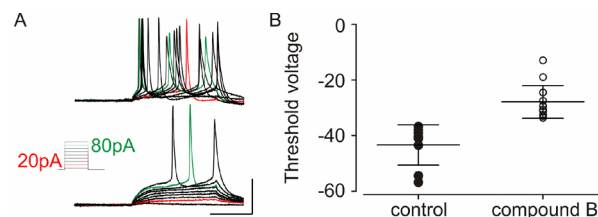

Figure 3. Effect of compound B on rat hippocampal neurons. (A) Representative recordings of cells treated with DMSO-containing vehicle (left) vs cells treated with 100 μM compound B (right). The inset shows the current clamp protocol of a series of 10 pA depolarizing current injections in which red and green indicate the current needed to elicit an action potential under control conditions (20 pA) and that of the treated cells (80 pA), respectively. (B) Average action potential thresholds are significantly higher in cells treated with compound B [-27.8 ± 1.6 mV (O); $n = 7$] than in cells treated with the DMSO-containing vehicle [-43.3 ± 2.4 mV ($\bullet$); $n = 7$].

ability of compound B to reduce the level of action potential firing in hippocampal neurons by shifting the firing threshold in the depolarizing direction, possibly by deferring $Na_v1.1$ channel activation to more positive membrane voltages (Figure 2B, Figure S5 of the Supporting Information, and Table 1). Subsequently, we examined the biological activity of this molecule in three established mouse epilepsy models.

Compound B Is Effective in Rodent Seizure Induction Paradigms. First, we tested compound B in the picrotoxin seizure induction assay, a widely used epilepsy model based on inhibiting GABA-mediated synaptic transmission. On the basis of the effective dose of rufinamide reported previously,[5] we tested compound B at a dose of 75 mg/kg. Even though the forelimb clonus (FC) tends to occur later in the compound B-treated mice, we observe no statistically significant differences between vehicle- and compound B-treated mice in their average latencies to the first myoclonic jerk (MJ) ($p = 0.4$) and FC ($p = 0.3$) (Figure 4). However, the average latency to the first generalized tonic-clonic seizure (GTCS) following treatment with compound B is significantly increased by 41% (1693 $\pm$ 315 s; $p = 0.03$) compared to that of vehicle-treated mice (1006 $\pm$ 106 s). There is no difference in the frequency of the behavioral seizures between the treatment groups.

Because one assay may not accurately reflect the ability of a drug to increase seizure resistance, we next investigated compound B efficacy in the fluorothyl paradigm, an established seizure induction model involving exposure of the animal to the volatile proconvulsant bis-2,2,2-trifluoroethyl ether.[43] Although the average latency to the MJ is comparable between vehicle- and compound B-treated mice ($p = 0.6$), the average latencies to the first GTCS and GTCS with hind limb extension (GTCS +) are increased by 43 and 56%, respectively ($p < 0.0001$; 652 $\pm$ 48 s for GTCS and 1155 $\pm$ 89 s for GTCS+), compared to those of the vehicle-treated group (281 $\pm$ 19 and 652 $\pm$ 38 s, respectively) (Figure 5). These results clearly demonstrate that compound B successfully increases the average latency to fluorothyl-induced GTCS and GTCS+.

Finally, we examined whether compound B is capable of reducing the occurrence and severity of seizures observed in the 6 Hz seizure induction paradigm, a model with a proven track record in drug development.[44] At a current intensity of 17 mA, 92% ($n = 22$ out of 24) of vehicle-treated mice display behavioral seizures and the majority of the observed seizures can be characterized as forelimb clonus (Racine score of 2) or rearing and falling (Racine score of 3) (Figure 5). In sharp
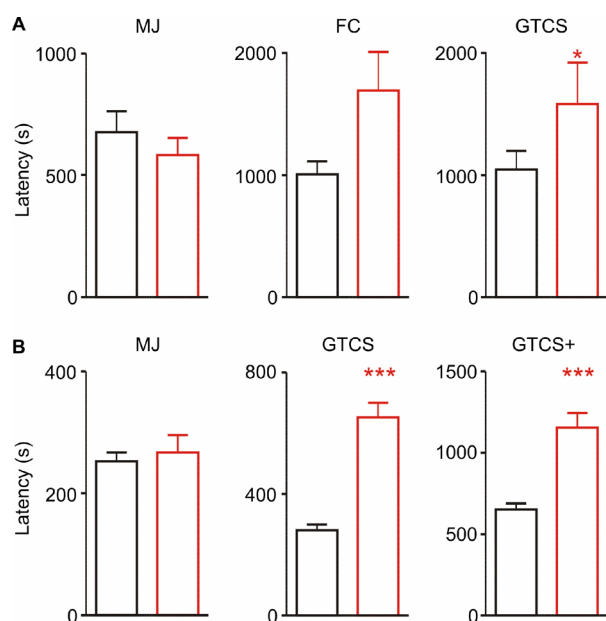
Figure 4. Compound B increases latencies to picrotoxin- and fluorothyl-induced generalized seizures. (A) Picrotoxin (10 mg/kg) was administered to vehicle-treated (black) and compound B-treated (red) male Crl:CF1 mice (75 mg/kg) 15 min prior to seizure induction. The average latencies in seconds to the first myoclonic jerk (MJ), forelimb clonus (FC), and generalized tonic-clonic seizure (GTCS) are compared. Compound B increases the average latency to the first GTCS. *$p < 0.05$. Error bars represent the standard error of the mean. (B) The latencies to the MJ, GTCS, and GTCS with hind limb extension (GTCS+) in the fluorothyl model are compared between vehicle-treated (black) and compound B-treated (red) male Crl:CF1 mice (75 mg/kg). The average latencies in seconds to the GTCS and GTCS+ are significantly longer in the compound B-treated mice. ***$p < 0.001$. Error bars represent the standard error of the mean.

contrast, only 29% ($n = 7$ out of 24; $p < 0.0001$) of the compound B-treated animals exhibit behavioral seizures, which are also dramatically less severe compared to those seen in the vehicle-treated mice ($p < 0.0001$). Overall, these results substantiate the notion that it is possible to achieve seizure resistance by modifying the *N*-benzyltriazole scaffold of rufinamide to target hNa$_v$1.1 activation.

■ DISCUSSION

The results presented here together with previously reported observations[15,16,33] suggest that the anti-epileptic drug rufinamide primarily targets the hNa$_v$1.1 and hNa$_v$1.6 isoforms in the brain (Figure 1 and Table 1). However, it is worth mentioning that additional mechanisms of action cannot be ruled out. For example, in an effort to find drugs for neuropathic pain, researchers found that rufinamide stabilizes the inactivated state of the Na$_v$1.7 isoform that is typically found in the peripheral nervous system.[33,45] Although this effect is rather small compared to that on hNa$_v$1.1 activation voltage, it may contribute to a beneficial effect of rufinamide in patients with febrile seizures.[46] Because anomalous hNa$_v$1.1 behavior has been implicated in LGS,[1,2,47−49] the therapeutic effects of rufinamide may indeed stem from its ability to shift the voltage dependence of activation of hNa$_v$1.1 channels to more positive potentials (Figure 1 and Table 1), a notion worth exploring for treating disorders involving hNa$_v$1.1 gain-of-function mutations

such as GEFS+,[10,14,18,50−53] migraine,[54,55] and post-traumatic stress disorder.[56] However, rufinamide may be contraindicated with patients in whom Na$_v$1.1 function is already impaired. For instance, Na$_v$1.1 deletion in mouse hippocampal and cortical interneurons decreases the level of sustained high-frequency firing of action potentials by reducing the overall sodium current without altering its voltage-dependent features.[28,57,58] Subsequently, loss of Na$_v$1.1 function may lead to hyperexcitability and epileptic seizures in patients with Dravet syndrome[58] and autism.[59,60] Although more experiments are needed to explain this phenomenon, it is worth noting that Na$_v$1.1 deletion in mice causes Na$_v$1.3 to be upregulated,[58] one of several observations that highlight a delicate balance between various signaling components involved in cellular excitation and inhibition that, in turn, complicates the translation of inhibitory anticonvulsant efficacy from heterologous expression systems to an intricate neuronal circuit.[11,15,35,36,61]
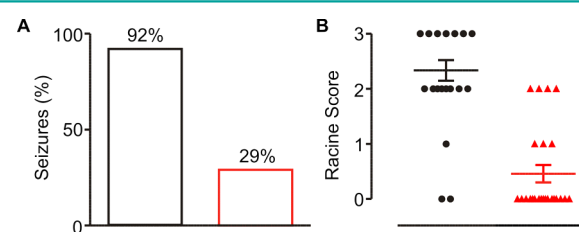
Figure 5. Compound B reduces the severity of seizures induced by the 6 Hz psychomotor paradigm. A current intensity of 17 mA was used to induce partial seizures in vehicle-treated (black) and compound B-treated (red) male Crl:CF1 mice (75 mg/kg). Following treatment with compound B, there is a 63% reduction in the number of mice exhibiting seizures (A; $p < 0.0001$). In addition, the seizures that were observed in the compound B-treated mice are typically less severe than those seen in the vehicle-treated mice (black) (B; $p < 0.0001$). Error bars represent the standard error of the mean.

Intrigued by the unique molecular organization of rufinamide (Figure 1A), we examined which features of the *N*-benzyltriazole core contribute most to its inhibitory effect on hNa$_v$1.1. As a result, three important features that need to be considered for hNa$_v$1.1 drug development using the *N*-benzyltriazole scaffold emerge from our SAR study. First, tweaking the electron density of the phenyl ring by removing or repositioning electron-withdrawing fluoro groups is a strategy worth exploring. Second, increasing triazole ring hydrophobicity by introducing alkyl substituents may give rise to molecules with better hNa$_v$1.1 efficacy. Third, an amide substituent on the triazole ring plays an important role in imparting hNa$_v$1.1 selectivity to rufinamide and its analogues. Considering these results, it will be very insightful to synthesize a series of rufinamide analogues bearing different alkyl chains in combination with varying electron density-altering substituents on the phenyl group and then test their efficacy as anti-epileptic agents. Subsequently, we identified a molecule with the properties mentioned above that does not influence hNa$_v$1.2, hNa$_v$1.3, or hNa$_v$1.6 activation or steady-state inactivation (compound B in Figure 2B) and examined its effect on Na$_v$1.1-expressing cultured hippocampal neurons (Figure 3). As anticipated when shifting the Na$_v$ channel activation voltage, we observed a significant increase in the action potential threshold (∼16 mV) in the presence of 100 μM compound B (Figure 3), an exciting result that motivated us to translate our findings to three rodent models of epilepsy. Consistent with a

role for $Na_v1.1$ in prompting neuronal firing, we found that compound B is capable of increasing the average latency to the GTCS in the picrotoxin (Figure 4) and fluorothyl paradigms (Figure 5). In addition, compound B reduces seizure occurrence and severity in the 6 Hz seizure induction assay (Figure 5), a model previously employed to successfully identify anticonvulsant drugs such as tiagabine,[62] vigabatrin,[62] and lacosamide.[63] Overall, these results demonstrate that modifying the unique *N*-benzyltriazole scaffold of rufinamide can produce biologically active molecules that target $hNa_v1.1$ opening, an outcome that may be exploited in the design of suitable compounds for investigating the functional role of $hNa_v1.1$ in healthy and diseased tissues or for treating $hNa_v1.1$-related gain-of-function disorders such as GEFS+[10,14,18,50−53] and migraine.[54,55] Consistent with the protection achieved in wild-type mice, compound B in particular may also find use as a general anticonvulsant. A more comprehensive interpretation of our results is that they provide a conceptual example for designing drugs that interact with specific Na_v channel isoforms, a necessary feature for reducing unwanted adverse effects.

■ METHODS

Channel Constructs. Human (h) $hNa_v1.1$ (NM_001165963.1), $hNa_v1.2$ (NM_021007.2), $hNa_v1.3$ (NM_006922.3), $hNa_v1.6$ (NM_014191.3), and $h\beta_1$ (NM_001037.4) clones were obtained from OriGene Technologies, Inc., and modified with an ER forwarding motif[25] and the $rNa_v1.2a$ 3′UTR region for expression in *Xenopus laevis* oocytes (acquired from *Xenopus* One). To check for undesired rearrangement events, the DNA sequence of all constructs was confirmed by automated DNA sequencing before further usage. cRNA was synthesized using T7 polymerase (Life Technologies) after the DNA had been linearized with the appropriate restriction enzymes.

Two-Electrode Voltage-Clamp Recording from *Xenopus* Oocytes. Channels were expressed in *Xenopus* oocytes together with β_1 in a 1:5 molar ratio, and currents were studied following incubation for 1−2 days after cRNA injection [incubated at 17 °C in 96 mM NaCl, 2 mM KCl, 5 mM HEPES, 1 mM $MgCl_2$, 1.8 mM $CaCl_2$, and 50 μg/mL gentamycin (pH 7.6) with NaOH] using two-electrode voltage-clamp recording techniques (OC-725C, Warner Instruments) with a 150 μL recording chamber. Heterologous $GABA_A$ receptor and hERG (Kv11.1) manipulations were achieved using previously reported procedures.[26,27] Nav channel data were filtered at 4 kHz and digitized at 20 kHz using pClamp10 software (Molecular Devices). Microelectrode resistances were 0.5−1 MΩ when the devices were filled with 3 M KCl. The external recording solution contained 100 mM NaCl, 5 mM HEPES, 1 mM $MgCl_2$, and 1.8 mM $CaCl_2$ (pH 7.6) with NaOH. All experiments were performed at room temperature (RT) (∼22 °C). Leak and background conductances, identified by blocking Na_v channels with tetrodotoxin, were subtracted for all of the Na_v channel-mediated currents. Chemicals and compounds A−D were obtained from Sigma-Aldrich, Vitasmlabs, and Maybridge (eMolecules).

Analysis of Channel Activity and Drug−Channel Interactions. Unless otherwise specified, voltage−activation relationships were obtained by measuring peak currents and calculating conductance (*G*), and a Boltzmann function was fit to the data according to the equation $G/G_{max} = [1 + e^{-zF(V-V_{1/2})/RT}]^{-1}$, where G/G_{max} is the normalized conductance, z is the equivalent charge, $V_{1/2}$ is the half-activation voltage, F is Faraday's constant, R is the gas constant, and T is the temperature in kelvin. Rufinamide and derivatives were dissolved in DMSO (∼5 mg mL^{-1} stock solution) and ad hoc diluted to a working concentration of 100 μM while taking great care not to reach the maximal solubility of the compounds. *Xenopus* oocytes expressing the various Na_v channel isoforms were incubated in solutions containing 100 μM drug (final DMSO concentration of ≤1%) for at least 1 h. We did not observe a significant alteration in drug-induced effects on Na_v channels between

1 h and overnight incubation. Differences in reported values were only considered significant when $p < 0.005$ (Student's *t* test). Off-line data analysis and statistical analysis were performed using Clampfit10 (Molecular Devices), Excel (Microsoft Office), and Origin 8 (OriginLab).

Action Potential Threshold Recordings in Hippocampal Neurons. Hippocampal neurons were dissected from Sprague-Dawley rat embryos on embryonic day 18. Cells were treated with papain (Worthington Biochemical), dissociated with a pipet, and plated over coverslips coated with collagen (Life Technologies) and poly-D-lysine (Sigma-Aldrich). Astrocyte beds were prepared at a density of 80000 cells/mL and cultured in DMEM (Life Technologies) with 10% fetal bovine serum and 6 mM glutamine for 14 days in 5% CO_2 at 37 °C. All of the medium was changed every week. Neurons were plated over confluent astrocyte beds at a density of 150000 cells/mL and cultured for 3 weeks in neurobasal medium (Life Technologies) supplemented with B27 and 2 mM glutaMAX. Half of the medium was changed every 3−4 days. Cells were treated for 3 h with compound B in 0.3% DMSO or a control (medium containing 0.3% DMSO) before recording. Coverslips were transferred to a chamber perfused at a rate of 2 mL/min at 32 °C with ACSF containing 140 mM NaCl, 5 mM KCl, 2 mM $CaCl_2$, 2 mM $MgCl_2$, 10 mM HEPES, and 10 mM glucose (pH 7.3 adjusted with NaOH). An Axopatch 200B instrument equipped with a Digidata 1440 digitizer and pClamp10 software were used. Whole-cell current clamp recordings were performed using borosilicate glass pipettes (4−6 MΩ) filled with a solution containing 135 mM potassium gluconate, 20 mM KCl, 10 mM HEPES, 4 mM Mg-ATP, 0.3 mM Na_2GTP, and 0.5 mM EGTA. Action potential thresholds were measured by a series of 100 ms, 10 pA depolarizing current injections. At the minimal current injection needed to elicit an action potential, the firing threshold was determined by calculating the potential at which the rate of rise crossed 40 V/s, using AxoGraph X. The input resistance was measured as the slope of the linear range of the current−voltage plot constructed from the steady-state voltage response to depolarizing current injections of 5 pA ranging from −40 to 0 pA with a duration of 500 ms. All cells measured were in the range of 300−500 MΩ, showing no significant difference between treatments (435 ± 38 MΩ for the control and 387 ± 32 MΩ for compound B with $n = 5$ for both sets of experiments). Data are presented as means ± the standard error of the mean. For statistical analysis, a Student's *t* test was performed using GraphPad Prism 6. The Johns Hopkins University Institutional Animal Care and Use Committee approved all experimental protocols involving rats.

Animal Husbandry and Drug Administration. Male Crl:CF1 mice (10−12 weeks old, Charles River) were housed under a 12 h light−dark cycle with free access to food and water, and all experiments were conducted between 10 a.m. and 4 p.m. 1-(Phenylmethyl)-1*H*-1,2,3-triazole-4-carboxamide-5-methyl (compound B) (Sigma-Aldrich) was suspended in a 40% solution of 2-hydroxypropyl-β-cyclodextrin (Sigma-Aldrich) in sterile saline (0.9%), and 15 min prior to each seizure induction paradigm, compound B (75 mg/kg) was administered via intraperitoneal (ip) injection. Vehicle-treated animals were similarly treated with 40% cyclodextrin and served as the controls for each experiment. The Emory University Institutional Animal Care and Use Committee approved all experimental protocols involving mice.

Seizure Induction Paradigms and Analyses. *Picrotoxin Seizure Induction.* Fifteen minutes prior to ip injection of picrotoxin (10 mg/kg, Sigma-Aldrich), mice were treated with the vehicle or compound B ($n = 12$ per group). Latencies to the first myoclonic jerk, forelimb clonus, and generalized tonic-clonic seizure were compared between compound B- and vehicle-treated mice. The myoclonic jerk is characterized by a sudden jerk of the upper body, whereas forelimb clonus involves rapid movement of the forelimbs for at least 5 s. Finally, the generalized tonic-clonic seizure involves the loss of postural control with rapid movement of the limbs for at least 5 s.

Fluorothyl Seizure Induction. Latencies to fluorothyl-induced seizures were determined as previously described.[28] Briefly, fluorothyl [2,2,2-trifluoroethyl ether (Sigma-Aldrich)] was dispensed at a rate of 20 μL/min into a Plexiglas chamber, and latencies to three behavioral

phenotypes were compared between vehicle-treated and compound B-treated (75 mg/kg) mice ($n = 12$ per group): (1) the first myoclonic jerk, (2) a generalized tonic-clonic seizure, and (3) a generalized tonic-clonic seizure with tonic extension. Similar to picrotoxin-mediated seizure induction, the myoclonic jerk is the first observable behavioral phenotype followed by the generalized tonic-clonic seizure that is characterized by a loss of postural control with rapid movement of all four limbs for at least 5 s. Lastly, the generalized tonic-clonic seizure with tonic hind limb extension involves the loss of postural control and rapid movement of all four limbs followed by downward extension of the limbs parallel to the body.

6 Hz Psychomotor Seizure Induction. Topical anesthetic (0.5% tetracaine hydrochloride ophthalmic solution) was applied to the cornea 30 min before testing. Fifteen minutes prior to seizure induction, mice were treated with the vehicle or compound B ($n = 12$ per group). Each mouse was manually restrained, and corneal stimulation (0.2 ms pulse, 6 Hz, 3 s) was performed at a current intensity of 17 mA (ECT Unit 57800, Ugo Basile, Comerio, Italy). The mice were observed for behavioral responses immediately following stimulation, and seizures were scored on the basis of a modified Racine scale: 0, no behavior; 1, staring; 2, forelimb clonus; 3, rearing and falling. The mice were randomized into two groups, and in the first trial, one group received the vehicle and the other compound B. The second trial was performed 1 week later, with each group receiving the opposite treatment. The resulting data were combined because no statistically significant differences were observed between the two trials.

Statistical Analysis. A Student's *t* test was used to identify statistically significant differences in latencies between vehicle- and compound B-treated groups for each seizure phenotype following administration of fluorothyl and picrotoxin. A Fisher Exact test was applied to determine differences in the percent of vehicle- and compound B-treated mice exhibiting seizures in the 6 Hz seizure induction paradigm, and a Wilcoxon matched-pairs signed rank test determined the differences in seizure severity. All data are presented as means ± the standard error of the mean; *p* values of <0.05 were considered significant.

ASSOCIATED CONTENT

Ⓢ Supporting Information
Gating characteristics of hNa$_v$1.1, hNa$_v$1.2, hNa$_v$1.3, and hNa$_v$1.6 (Figure S1), effect of DMSO on hNa$_v$ channel isoforms (Figure S2), effect of rufinamide derivatives on hNa$_v$1.1 (Figure S3), evidence of the fact that rufinamide and compound B do not affect hNa$_v$1.1 persistent current or activate the $\alpha1/\beta2/\gamma2$ GABAA receptor (Figure S4), evidence that compound B does not influence the tested gating properties of other neuronal Na$_v$ channel isoforms (Figure S5), evidence that rufinamide and compound B do not influence hNa$_v$1.1 slow inactivation (Figure S6), evidence that rufinamide and compound B do not inhibit hERG channels (Figure S7), lack of an effect of compound B on the tested gating properties of hNa$_v$1.2, hNa$_v$1.3, and hNa$_v$1.6 (Table S1), and evidence that rufinamide and compound B do not influence hNa$_v$1.1 slow inactivation (Table S2). This material is available free of charge via the Internet at http://pubs.acs.org.

AUTHOR INFORMATION

Corresponding Authors
*E-mail: aescayg@emory.edu.
*E-mail: frankbosmans@jhmi.edu.

Author Contributions
J.G., S.D., and M.D.-B. contributed equally to this work.

Notes
The authors declare no competing financial interest.

REFERENCES
(1) Trevathan, E., Murphy, C. C., and Yeargin-Allsopp, M. (1997) Prevalence and descriptive epidemiology of Lennox-Gastaut syndrome among Atlanta children. *Epilepsia 38*, 1283−1288.
(2) Arzimanoglou, A., French, J., Blume, W. T., Cross, J. H., Ernst, J. P., Feucht, M., Genton, P., Guerrini, R., Kluger, G., Pellock, J. M., Perucca, E., and Wheless, J. W. (2009) Lennox-Gastaut syndrome: A consensus approach on diagnosis, assessment, management, and trial methodology. *Lancet Neurol. 8*, 82−93.
(3) Brodie, M. J., Rosenfeld, W. E., Vazquez, B., Sachdeo, R., Perdomo, C., Mann, A., and Arroyo, S. (2009) Rufinamide for the adjunctive treatment of partial seizures in adults and adolescents: A randomized placebo-controlled trial. *Epilepsia 50*, 1899−1909.
(4) Deeks, E. D., and Scott, L. J. (2006) Rufinamide. *CNS Drugs 20*, 751−760 , 761 (discussion).
(5) White, H. S., Franklin, M. R., Kupferberg, H. J., Schmutz, M., Stables, J. P., and Wolf, H. H. (2008) The anticonvulsant profile of rufinamide (CGP 33101) in rodent seizure models. *Epilepsia 49*, 1213−1220.
(6) Coppola, G., Zamponi, N., Kluger, G., Mueller, A., Anna Rita, M., Parisi, P., Isone, C., Santoro, E., Curatolo, P., and Verrotti, A. (2012) Rufinamide for refractory focal seizures: An open-label, multicenter European study. *Seizure 22*, 33−36.
(7) Critchley, D. J., Aluri, J., Boyd, P., Whayman, M., Narurkar, M., Delargy, H., and Bibbiani, F. (2011) Bioavailability of three rufinamide oral suspensions compared with the marketed 400-mg tablet formulation: Results from a randomized-sequence, open-label, four-period, four-sequence crossover study in healthy subjects. *Clin. Ther. 33*, 146−157.
(8) May, T. W., Boor, R., Rambeck, B., Jurgens, U., Korn-Merker, E., and Brandt, C. (2011) Serum concentrations of rufinamide in children and adults with epilepsy: The influence of dose, age, and comedication. *Ther. Drug Monit. 33*, 214−221.
(9) Catterall, W. A., Goldin, A. L., and Waxman, S. G. (2005) International Union of Pharmacology. XLVII. Nomenclature and structure-function relationships of voltage-gated sodium channels. *Pharmacol. Rev. 57*, 397−409.
(10) Escayg, A., and Goldin, A. L. (2010) Sodium channel SCN1A and epilepsy: Mutations and mechanisms. *Epilepsia 51*, 1650−1658.
(11) Mantegazza, M., Curia, G., Biagini, G., Ragsdale, D. S., and Avoli, M. (2010) Voltage-gated sodium channels as therapeutic targets in epilepsy and other neurological disorders. *Lancet Neurol. 9*, 413−424.
(12) Ragsdale, D. S. (2008) How do mutant Nav1.1 sodium channels cause epilepsy? *Brain Res. Rev. 58*, 149−159.
(13) Oliva, M., Berkovic, S. F., and Petrou, S. (2012) Sodium channels and the neurobiology of epilepsy. *Epilepsia 53*, 1849−1859.
(14) Catterall, W. A. (2014) Sodium channels, inherited epilepsy, and antiepileptic drugs. *Annu. Rev. Pharmacol. Toxicol. 54*, 317−338.

(15) McLean, M. J., Schmutz, M., Pozza, M. F., and Wamil, A. W. (2005) Effects of rufinamide on sodium-dependent action potential firing and sodium currents of rodent central neurons. *Epilepsia 46*, 375−375.

(16) Niespodziany, I., Leclere, N., Vandenplas, C., Foerch, P., and Wolff, C. (2013) Comparative study of lacosamide and classical sodium channel blocking antiepileptic drugs on sodium channel slow inactivation. *J. Neurosci. Res. 91*, 436−443.

(17) Whitaker, W. R., Clare, J. J., Powell, A. J., Chen, Y. H., Faull, R. L., and Emson, P. C. (2000) Distribution of voltage-gated sodium channel α-subunit and β-subunit mRNAs in human hippocampal formation, cortex, and cerebellum. *J. Comp. Neurol. 422*, 123−139.

(18) Catterall, W. A., Kalume, F., and Oakley, J. C. (2010) NaV1.1 channels and epilepsy. *J. Physiol. 588*, 1849−1859.

(19) Escayg, A., MacDonald, B. T., Meisler, M. H., Baulac, S., Huberfeld, G., An-Gourfinkel, I., Brice, A., LeGuern, E., Moulard, B., Chaigne, D., Buresi, C., and Malafosse, A. (2000) Mutations of SCN1A, encoding a neuronal sodium channel, in two families with GEFS+2. *Nat. Genet. 24*, 343−345.

(20) Papale, L. A., Beyer, B., Jones, J. M., Sharkey, L. M., Tufik, S., Epstein, M., Letts, V. A., Meisler, M. H., Frankel, W. N., and Escayg, A. (2009) Heterozygous mutations of the voltage-gated sodium channel SCN8A are associated with spike-wave discharges and absence epilepsy in mice. *Hum. Mol. Genet. 18*, 1633−1641.

(21) Veeramah, K. R., O'Brien, J. E., Meisler, M. H., Cheng, X., Dib-Hajj, S. D., Waxman, S. G., Talwar, D., Girirajan, S., Eichler, E. E., Restifo, L. L., Erickson, R. P., and Hammer, M. F. (2012) De novo pathogenic SCN8A mutation identified by whole-genome sequencing of a family quartet affected by infantile epileptic encephalopathy and SUDEP. *Am. J. Hum. Genet. 90*, 502−510.

(22) Hains, B. C., and Waxman, S. G. (2007) Sodium channel expression and the molecular pathophysiology of pain after SCI. *Prog. Brain Res. 161*, 195−203.

(23) Estacion, M., Gasser, A., Dib-Hajj, S. D., and Waxman, S. G. (2010) A sodium channel mutation linked to epilepsy increases ramp and persistent current of Nav1.3 and induces hyperexcitability in hippocampal neurons. *Exp. Neurol. 224*, 362−368.

(24) Vanoye, C. G., Gurnett, C. A., Holland, K. D., George, A. L., Jr., and Kearney, J. A. (2014) Novel SCN3A variants associated with focal epilepsy in children. *Neurobiol. Dis. 62*, 313−322.

(25) O'Kelly, I., Butler, M. H., Zilberberg, N., and Goldstein, S. A. (2002) Forward transport. 14-3-3 binding overcomes retention in endoplasmic reticulum by dibasic signals. *Cell 111*, 577−588.

(26) Boileau, A. J., Kucken, A. M., Evers, A. R., and Czajkowski, C. (1998) Molecular dissection of benzodiazepine binding and allosteric coupling using chimeric γ-aminobutyric acidA receptor subunits. *Mol. Pharmacol. 53*, 295−303.

(27) Trudeau, M. C., Warmke, J. W., Ganetzky, B., and Robertson, G. A. (1995) HERG, a human inward rectifier in the voltage-gated potassium channel family. *Science 269*, 92−95.

(28) Dutton, S. B., Makinson, C. D., Papale, L. A., Shankar, A., Balakrishnan, B., Nakazawa, K., and Escayg, A. (2012) Preferential inactivation of Scn1a in parvalbumin interneurons increases seizure susceptibility. *Neurobiol. Dis. 49C*, 211−220.

(29) Burbidge, S. A., Dale, T. J., Powell, A. J., Whitaker, W. R., Xie, X. M., Romanos, M. A., and Clare, J. J. (2002) Molecular cloning, distribution and functional analysis of the NA(V)1.6. Voltage-gated sodium channel from human brain. *Brain Research. Molecular Brain Research 103*, 80−90.

(30) Chen, Y. H., Dale, T. J., Romanos, M. A., Whitaker, W. R., Xie, X. M., and Clare, J. J. (2000) Cloning, distribution and functional analysis of the type III sodium channel from human brain. *Eur. J. Neurosci. 12*, 4281−4289.

(31) Mantegazza, M., Yu, F. H., Powell, A. J., Clare, J. J., Catterall, W. A., and Scheuer, T. (2005) Molecular determinants for modulation of persistent sodium current by G-protein betagamma subunits. *J. Neurosci. 25*, 3341−3349.

(32) Xie, X., Dale, T. J., John, V. H., Cater, H. L., Peakman, T. C., and Clare, J. J. (2001) Electrophysiological and pharmacological properties of the human brain type IIA Na+ channel expressed in a stable mammalian cell line. *Pfluegers Arch. 441*, 425−433.

(33) Suter, M. R., Kirschmann, G., Laedermann, C. J., Abriel, H., and Decosterd, I. (2013) Rufinamide Attenuates Mechanical Allodynia in a Model of Neuropathic Pain in the Mouse and Stabilizes Voltage-gated Sodium Channel Inactivated State. *Anesthesiology 118*, 160−172.

(34) Ledwell, J. L., and Aldrich, R. W. (1999) Mutations in the S4 region isolate the final voltage-dependent cooperative step in potassium channel activation. *J. Gen. Physiol. 113*, 389−414.

(35) Kwan, P., Sills, G. J., and Brodie, M. J. (2001) The mechanisms of action of commonly used antiepileptic drugs. *Pharmacol. Ther. 90*, 21−34.

(36) Lipkind, G. M., and Fozzard, H. A. (2010) Molecular model of anticonvulsant drug binding to the voltage-gated sodium channel inner pore. *Mol. Pharmacol. 78*, 631−638.

(37) Rogawski, M. A. (2006) Diverse mechanisms of antiepileptic drugs in the development pipeline. *Epilepsy Res. 69*, 273−294.

(38) Chao, T. I., and Alzheimer, C. (1995) Effects of phenytoin on the persistent Na+ current of mammalian CNS neurones. *NeuroReport 6*, 1778−1780.

(39) Arroyo, S. (2007) Rufinamide. *Neurotherapeutics 4*, 155−162.

(40) Mohler, H. (2006) GABA(A) receptor diversity and pharmacology. *Cell Tissue Res. 326*, 505−516.

(41) Trimmer, J. S., and Rhodes, K. J. (2004) Localization of voltage-gated ion channels in mammalian brain. *Annu. Rev. Physiol. 66*, 477−519.

(42) Sievers, F., Wilm, A., Dineen, D., Gibson, T. J., Karplus, K., Li, W., Lopez, R., McWilliam, H., Remmert, M., Soding, J., Thompson, J. D., and Higgins, D. G. (2011) Fast, scalable generation of high-quality protein multiple sequence alignments using Clustal Omega. *Mol. Syst. Biol. 7*, 539.

(43) Applegate, C. D., Samoriski, G. M., and Ozduman, K. (1997) Effects of valproate, phenytoin, and MK-801 in a novel model of epileptogenesis. *Epilepsia 38*, 631−636.

(44) Barton, M. E., Klein, B. D., Wolf, H. H., and White, H. S. (2001) Pharmacological characterization of the 6 Hz psychomotor seizure model of partial epilepsy. *Epilepsy Res. 47*, 217−227.

(45) Ahmad, S., Dahllund, L., Eriksson, A. B., Hellgren, D., Karlsson, U., Lund, P. E., Meijer, I. A., Meury, L., Mills, T., Moody, A., Morinville, A., Morten, J., O'Donnell, D., Raynoschek, C., Salter, H., Rouleau, G. A., and Krupp, J. J. (2007) A stop codon mutation in SCN9A causes lack of pain sensation. *Hum. Mol. Genet. 16*, 2114−2121.

(46) Singh, N. A., Pappas, C., Dahle, E. J., Claes, L. R., Pruess, T. H., De Jonghe, P., Thompson, J., Dixon, M., Gurnett, C., Peiffer, A., White, H. S., Filloux, F., and Leppert, M. F. (2009) A role of SCN9A in human epilepsies, as a cause of febrile seizures and as a potential modifier of Dravet syndrome. *PLoS Genet. 5*, e1000649.

(47) Glauser, T., Kluger, G., Sachdeo, R., Krauss, G., Perdomo, C., and Arroyo, S. (2008) Rufinamide for generalized seizures associated with Lennox-Gastaut syndrome. *Neurology 70*, 1950−1958.

(48) Hancock, E. C., and Cross, H. H. (2009) Treatment of Lennox-Gastaut syndrome. *Cochrane Database of Systematic Reviews*, CD003277.

(49) Selmer, K. K., Lund, C., Brandal, K., Undlien, D. E., and Brodtkorb, E. (2009) SCN1A mutation screening in adult patients with Lennox-Gastaut syndrome features. *Epilepsy & Behavior 16*, 555−557.

(50) Claes, L. R., Deprez, L., Suls, A., Baets, J., Smets, K., Van Dyck, T., Deconinck, T., Jordanova, A., and De Jonghe, P. (2009) The SCN1A variant database: A novel research and diagnostic tool. *Hum. Mutat. 30*, E904−E920.

(51) Spampanato, J., Kearney, J. A., de Haan, G., McEwen, D. P., Escayg, A., Aradi, I., MacDonald, B. T., Levin, S. I., Soltesz, I., Benna, P., Montalenti, E., Isom, L. L., Goldin, A. L., and Meisler, M. H. (2004) A novel epilepsy mutation in the sodium channel SCN1A identifies a cytoplasmic domain for β subunit interaction. *J. Neurosci. 24*, 10022−10034.

1211

dx.doi.org/10.1021/cb500108p | *ACS Chem. Biol.* 2014, 9, 1204−1212

(52) Volkers, L., Kahlig, K. M., Verbeek, N. E., Das, J. H., van Kempen, M. J., Stroink, H., Augustijn, P., van Nieuwenhuizen, O., Lindhout, D., George, A. L., Jr., Koeleman, B. P., and Rook, M. B. (2011) Nav 1.1 dysfunction in genetic epilepsy with febrile seizures-plus or Dravet syndrome. *Eur. J. Neurosci. 34*, 1268−1275.

(53) Lossin, C. (2009) A catalog of SCN1A variants. *Brain Dev. 31*, 114−130.

(54) Dichgans, M., Freilinger, T., Eckstein, G., Babini, E., Lorenz-Depiereux, B., Biskup, S., Ferrari, M. D., Herzog, J., van den Maagdenberg, A. M., Pusch, M., and Strom, T. M. (2005) Mutation in the neuronal voltage-gated sodium channel SCN1A in familial hemiplegic migraine. *Lancet 366*, 371−377.

(55) Cestele, S., Labate, A., Rusconi, R., Tarantino, P., Mumoli, L., Franceschetti, S., Annesi, G., Mantegazza, M., and Gambardella, A. (2013) Divergent effects of the T1174S SCN1A mutation associated with seizures and hemiplegic migraine. *Epilepsia 54*, 927−935.

(56) Moran, M., and Woiwode, T. (2009) Rufinamide for the Treatment of Post-Traumatic Stress Disorder. U.S. Patent 20090054414 A1.

(57) Oakley, J. C., Kalume, F., Yu, F. H., Scheuer, T., and Catterall, W. A. (2009) Temperature- and age-dependent seizures in a mouse model of severe myoclonic epilepsy in infancy. *Proc. Natl. Acad. Sci. U.S.A. 106*, 3994−3999.

(58) Yu, F. H., Mantegazza, M., Westenbroek, R. E., Robbins, C. A., Kalume, F., Burton, K. A., Spain, W. J., McKnight, G. S., Scheuer, T., and Catterall, W. A. (2006) Reduced sodium current in GABAergic interneurons in a mouse model of severe myoclonic epilepsy in infancy. *Nat. Neurosci. 9*, 1142−1149.

(59) Han, S., Tai, C., Westenbroek, R. E., Yu, F. H., Cheah, C. S., Potter, G. B., Rubenstein, J. L., Scheuer, T., de la Iglesia, H. O., and Catterall, W. A. (2012) Autistic-like behaviour in Scn1a± mice and rescue by enhanced GABA-mediated neurotransmission. *Nature 489*, 385−390.

(60) Weiss, L. A., Escayg, A., Kearney, J. A., Trudeau, M., MacDonald, B. T., Mori, M., Reichert, J., Buxbaum, J. D., and Meisler, M. H. (2003) Sodium channels SCN1A, SCN2A and SCN3A in familial autism. *Mol. Psychiatry 8*, 186−194.

(61) Rogawski, M. A., and Loscher, W. (2004) The neurobiology of antiepileptic drugs. *Nat. Rev. Neurosci. 5*, 553−564.

(62) Rowley, N. M., and White, H. S. (2010) Comparative anticonvulsant efficacy in the corneal kindled mouse model of partial epilepsy: Correlation with other seizure and epilepsy models. *Epilepsy Res. 92*, 163−169.

(63) Stohr, T., Kupferberg, H. J., Stables, J. P., Choi, D., Harris, R. H., Kohn, H., Walton, N., and White, H. S. (2007) Lacosamide, a novel anti-convulsant drug, shows efficacy with a wide safety margin in rodent models for epilepsy. *Epilepsy Res. 74*, 147−154.